



**HAL**  
open science

## Design and characterization of a chitosan-enriched fibrin hydrogel for human dental pulp regeneration

Maxime Ducret, Alexandra Montembault, Jérôme Josse, Marielle Padeloup, Alexis Celle, Rafiq Benchrih, Frédéric Mallein-Gerin, Brigitte Alliot-Licht, Laurent David, Jean-Christophe Farges

### ► To cite this version:

Maxime Ducret, Alexandra Montembault, Jérôme Josse, Marielle Padeloup, Alexis Celle, et al.. Design and characterization of a chitosan-enriched fibrin hydrogel for human dental pulp regeneration. Dental Materials, 2019, 35 (4), pp.523-533. 10.1016/j.dental.2019.01.018 . hal-02378443

**HAL Id: hal-02378443**

**<https://hal.science/hal-02378443>**

Submitted on 22 Oct 2021

**HAL** is a multi-disciplinary open access archive for the deposit and dissemination of scientific research documents, whether they are published or not. The documents may come from teaching and research institutions in France or abroad, or from public or private research centers.

L'archive ouverte pluridisciplinaire **HAL**, est destinée au dépôt et à la diffusion de documents scientifiques de niveau recherche, publiés ou non, émanant des établissements d'enseignement et de recherche français ou étrangers, des laboratoires publics ou privés.



Distributed under a Creative Commons Attribution - NonCommercial 4.0 International License

## Design and characterization of a chitosan-enriched fibrin hydrogel for human dental pulp regeneration

*Maxime Ducret<sup>a,b,c</sup>, Alexandra Montembault<sup>d</sup>, Jérôme Josse<sup>e</sup>, Marielle Padeloup<sup>a</sup>, Alexis Celle<sup>a</sup>, Rafiqqa Benchrih<sup>d</sup>, Frédéric Mallein-Gerin<sup>a</sup>, Brigitte Alliot-Licht<sup>f,g,h</sup>, Laurent David<sup>d</sup>, Jean-Christophe Farges<sup>a,b,c,\*</sup>*

<sup>a</sup> *Laboratoire de Biologie Tissulaire et Ingénierie thérapeutique, UMR5305 CNRS/Université Lyon 1, UMS3444 BioSciences Gerland-Lyon Sud, Lyon, France*

<sup>b</sup> *Université de Lyon, Université Lyon 1, Faculté d'Odontologie, Lyon, France*

<sup>c</sup> *Hospices Civils de Lyon, Service d'Odontologie, Lyon, France*

<sup>d</sup> *Université de Lyon, Université Lyon 1, CNRS, Ingénierie des Matériaux Polymères (IMP), UMR5223, Villeurbanne, France*

<sup>e</sup> *CIRI - Centre International de Recherche en Infectiologie, INSERM U1111/CNRS UMR5308/ENS Lyon/Université Lyon 1, Lyon, France*

<sup>f</sup> *Centre de Recherche en Transplantation et Immunologie, INSERM UMR1064, Université de Nantes, Nantes, France*

<sup>g</sup> *Université de Nantes, Faculté d'Odontologie, Nantes, France*

<sup>h</sup> *CHU de Nantes, Service d'Odontologie Conservatrice et Pédiatrique, Nantes, France*

*\*Corresponding author at: Laboratoire de Biologie Tissulaire et Ingénierie thérapeutique, UMR5305 CNRS/UCBL, Institut de Biologie et Chimie des Protéines, 7 passage du Vercors, 69367 Lyon Cedex 07, France.*

E-mail address: [jean-christophe.farges@univ-lyon1.fr](mailto:jean-christophe.farges@univ-lyon1.fr) (J.-C. Farges).

Short title: Fibrin-chitosan scaffold for pulp regeneration

**Keywords:** Regenerative dentistry; Tissue engineering; Hydrogel; Fibrin; Chitosan; Antibacterial effect; Dental pulp mesenchymal stem/stromal cells; Cell viability; Proliferation; Collagen synthesis

1 **ABSTRACT**

2 *Objective.* Regenerating a functional dental pulp in the pulpectomized root canal has  
3 been recently proposed as a novel therapeutic strategy in dentistry. To reach this goal,  
4 designing an appropriate scaffold able to prevent the growth of residual endodontic  
5 bacteria, while supporting dental pulp tissue neoformation, is needed. Our aim was to  
6 create an innovative cellularized fibrin hydrogel supplemented with chitosan to confer  
7 this hydrogel antibacterial property.

8 *Methods.* Several fibrin-chitosan formulations were first screened by rheological  
9 analyses, and the most appropriate for clinical use was then studied in terms of  
10 microstructure (by scanning electron microscopy), antimicrobial effect (analysis of  
11 *Enterococcus faecalis* growth), dental pulp-mesenchymal stem/stromal cell (DP-MS-C)  
12 viability and spreading after 7 days of culture (LiveDead® test), DP-MS-C ultrastructure  
13 and extracellular matrix deposition (transmission electron microscopy), and DP-MS-C  
14 proliferation and collagen production (RT-qPCR and immunohistochemistry).

15 *Results.* A formulation associating 10 mg/mL fibrinogen and 0.5% (w/w), 40% degree of  
16 acetylation, medium molar mass chitosan was found to be relevant in order to forming a  
17 fibrin-chitosan hydrogel at cytocompatible pH (# 7.2). Comparative analysis of fibrin-  
18 alone and fibrin-chitosan hydrogels revealed a potent antibacterial effect of the chitosan  
19 in the fibrin network, and similar DP-MS-C viability, fibroblast-like morphology,  
20 proliferation rate and type I/III collagen production capacity.

21 *Significance.* These results indicate that incorporating chitosan within a fibrin hydrogel  
22 would be beneficial to promote human DP tissue neoformation thanks to chitosan  
23 antibacterial effect and the absence of significant detrimental effect of chitosan on dental  
24 pulp cell morphology, viability, proliferation and collagenous matrix production.

25

---

## 1. Introduction

Previous studies have shown that the survival rate is lower for endodontically-treated teeth compared to their living counterparts. This has been attributed to the absence of the dental pulp (DP) immune defence, sensory system, and repair/regenerative capacity which makes the tooth more susceptible to re-infection and/or fracture [1,2]. In this context, therapeutic strategies aiming at regenerating a functional DP in the devitalized endodontic space recently received great attention [3-7]. Among the various approaches tested, the cell-based regenerative one has given promising results [8]. This approach relies on the injection, into the endodontic space, of a cellular product made of stem/precursor cells embedded in a tridimensional scaffold, functionalized or not with bioactive molecules. Important clinical and biological requirements for a cellularized scaffold to be used in DP regeneration include easy handling allowing for a rapid implantation into the endodontic space by the dental practitioner (within minutes), low viscosity for a good injectability into such a small-sized space, antibacterial properties to prevent the growth of residual endodontic bacteria, physiological degradation by host and/or encapsulated cells, and rapid replacement with an extracellular matrix (ECM) characteristic of the DP tissue. Numerous kinds of scaffolds have been tested including natural and synthetic polymers/co-polymers, hydroxyapatite/tricalcium phosphate powders, self-assembling peptide systems, and platelet-rich plasma [9-14]. So far, none of these scaffolds was found to possess the structural and functional properties of an ideal biomaterial for DP regeneration, and designing innovative formulations is clearly required [7,10,15].

Fibrin is a natural, insoluble protein which is produced following fibrinogen polymerization under thrombin control during blood clot formation. It forms a fibrous

51 network important for hemostasis and subsequent wound healing [16]. Used as a  
52 scaffold, fibrin was recently found to be highly suitable for DP regeneration since it  
53 clearly supports pulp-like tissue formation [17]. Its advantages include excellent  
54 cytocompatibility and physiological degradation kinetics, non-toxicity of degradation  
55 products, and replacement with cell-derived ECM within a few days [18]. Mechanical  
56 properties of fibrin scaffolds can be easily fine-tuned by controlling fibrinogen  
57 concentration and ionic strength, in order to obtain (i) viscoelastic properties similar to  
58 that of connective tissue ECM, (ii) fast diffusion of nutrients and metabolites, and (iii)  
59 homogeneous cell encapsulation [18]. However, the absence of antibacterial activity of  
60 fibrin or of its by-products during the degradation process [19] may constitute an  
61 important limitation, because microorganisms remaining in the endodontic space and  
62 dentin tubules may hinder the DP regeneration process [20-22]. This limitation could be  
63 overcome by incorporating antibacterial agents to the fibrin scaffold. Among these,  
64 chitosan has received considerable attention for over 30 years [23,24]. Chitosan is a  
65 natural polysaccharide biopolymer obtained by N-deacetylation of chitin, a major  
66 structural component of the exoskeleton of arthropods and insects, the endoskeleton of  
67 cephalopods, and fungal cell walls [25]. It is known to possess antimicrobial activity  
68 against a variety of gram-negative and gram-positive bacteria, including *Enterococcus*  
69 *fæcalis*, a pathogen frequently found in persistent root canal infections [25-28].  
70 Mechanisms responsible for this activity are not fully understood but may include: the  
71 interference of the positively charged chitosan molecules with the negatively charged residues  
72 on the bacterial surface, the interaction of diffused hydrolysis products with microbial DNA  
73 (which leads to the inhibition of the mRNA and protein synthesis), the chelation of nutrients  
74 and essential metals, and the formation of a polymer membrane on the cell surface which  
75 prevents nutrients or oxygen from entering the cell [29]. Chitosan could thus be a good

76 candidate as an antibacterial agent, provided that it keeps its antimicrobial properties  
77 upon incorporation into the fibrin scaffold.

78 The aim of this study was to design an injectable hydrogel-type scaffold  
79 associating fibrin and chitosan in a formulation which preserves chitosan antibacterial  
80 properties, while not affecting dental pulp-mesenchymal stem/stromal cell (DP-MS) cell  
81 viability, spreading and proliferation, and DP-like ECM deposition within the hydrogel.

82

---

## 83 **2. Materials and methods**

84

### 85 *2.1. Reagents*

86

87 Human fibrinogen (ref. F3879) and thrombin (ref. T6884) were purchased from Sigma-  
88 Aldrich (Saint-Louis, USA), and highly deacetylated shrimp shell chitosan (batch type  
89 243) from Mahtani Chitosan® (Gujarat, India). The chemically defined cell culture  
90 medium SPE-IV/EBM® and human placental collagens I and III were obtained from  
91 ABCellBio (Paris, France), the anti-MKI67 rabbit recombinant monoclonal antibody  
92 (clone SP6, ref. M3062) from Eurobio (Courtabœuf, France), the anti-type I collagen  
93 rabbit polyclonal antibody (ref. 20111[380k]) and the anti-type III collagen mouse  
94 monoclonal antibody (clone 8D1-8C7, ref. 60315[316f]) from Novotec (Bron, France).

95

### 96 *2.2. Preparation and characterization of the chitosan solution, fibrin hydrogels and* 97 *fibrin-chitosan hydrogels*

98

99 The commercial chitosan was dissolved and filtered successively through 3, 0.8 and 0.45  
100 µm Millipore® membranes to obtain a high-purity material [30] which was

101 characterized by  $^1\text{H}$  nuclear magnetic resonance (NMR) spectroscopy and size exclusion  
102 chromatography coupled online with a differential refractometer (Wyatt Optilab T-rEx)  
103 and a multi angle laser light scattering detector (Wyatt HELEOS) [31]. Results indicated  
104 that this chitosan had an initial degree of acetylation (DA) of  $1.5 \pm 0.2 \%$  and a weight-  
105 average molar mass ( $M_w$ ) of  $160 \pm 10 \text{ kg/mol}$  with a dispersity index  $\mathcal{D}$  of  $1.9 \pm 0.2$  ( $\mathcal{D} =$   
106  $M_w / M_n$ ). This polymer was then N-reacetylated to reach a DA of 40% using acetic  
107 anhydride as a reactive, as previously described [32]. Briefly, chitosan was dissolved at a  
108 concentration of 0.5% (w/v) in a water/1,2-propanediol mixture (1/1 [v/v]). Acetic  
109 anhydride was then diluted in 1,2-propanediol and this resulting acetylating reactive  
110 was added dropwise to the chitosan solution. The amount of acetic anhydride added  
111 corresponded to the stoichiometric amount necessary to achieve the required degree of  
112 acetylation. The medium was let to stand for 3 h. The N-reacetylated chitosan was then  
113 isolated by precipitation with aqueous ammonia, thoroughly washed with deionized  
114 water until neutral pH, and freeze-dried.

115 For the fibrin-chitosan hydrogel preparation, a 1% [w/w] DA40% chitosan  
116 solution was prepared by dissolving overnight the lyophilized polymer powder in a  
117 deionized aqueous solution of acetic acid. The quantity of acid added corresponded to  
118 the amount necessary to reach the protonation of the free amine site of D-glucosamine  
119 residues in the aqueous acidic solution. The pH of the chitosan solution was then  
120 increased to a cytocompatible level (7.1-7.2) by adding sodium hydroxide while  
121 avoiding chitosan precipitation. The final chitosan solution was sterilized by autoclaving  
122 at  $121^\circ\text{C}$  for 20 minutes. The viscosity of 0.2-1% chitosan solutions was then assessed in  
123 a static mode with an AR2000 rheometer (TA instruments, New Castle, DE, USA), by  
124 using a coaxial cylinder-cylinder geometry (Couette geometry) with a temperature fixed

125 at 298 K and a shear rate varying between  $10^{-3} \text{ s}^{-1}$  and  $50 \text{ s}^{-1}$ . The viscosity value  $\eta_0$  was  
126 determined from the Newtonian plateau at low shear rates.

127 Several fibrin-chitosan formulations were then prepared by mixing solutions of  
128 80 mg/mL fibrinogen, 3 M sodium chloride, 0.4 M calcium chloride, 1% chitosan, and 4  
129 U/mL thrombin, in appropriate proportions to obtain fibrin and chitosan final  
130 concentrations of 10 mg/mL and 0.1-0.5%, respectively, into the hydrogel. The  
131 viscoelastic behavior of these formulations was investigated in a dynamic mode by using  
132 a 25 mm parallel plate geometry. The linear domain was determined by a strain sweep  
133 test at an angular frequency of 10 rad/s. The strain amplitude was then fixed at 1 %.  
134 Measurements of storage and loss moduli were then performed over time to evaluate  
135 the crossing point between these two moduli, indicative of the gel point.

136 For fibrin-alone and fibrin-chitosan hydrogel characterization with scanning  
137 electron microscopy, samples were prepared by mixing solutions of 80 mg/mL  
138 fibrinogen, 3 M sodium chloride, 0.4 M calcium chloride, phosphate-buffered saline  
139 (PBS; for fibrin-alone hydrogels) or 1% chitosan (for fibrin-chitosan hydrogels), and  
140 finally 4 U/mL thrombin, in appropriate proportions to obtain fibrin and chitosan final  
141 concentrations of 10 mg/mL and 0.5%, respectively, into the hydrogel. 35  $\mu\text{L}$  of the mix  
142 were then injected into small cylindrical-conical plastic molds (7 mm long and 1-1.5 mm  
143 wide). After gelation, molds containing hydrogels were placed in 24-well dishes and  
144 covered with the SPE-IV/EBM<sup>®</sup> medium used for experiments with DP-MSC-populated  
145 hydrogels. Hydrogels were maintained in this medium for 7 days, and then fixed in 2%  
146 glutaraldehyde in 0.1 M sodium cacodylate buffer at room temperature (RT) for 4 h.  
147 After washing, samples were post-fixed in 1% osmium tetroxide for 1 h, dehydrated by  
148 critical point drying (CPD300; Leica, Solms, Germany), mounted on aluminum stubs,  
149 sputter-coated with a layer of copper using a MED020 sputter coater (Oerlikon Balzers,



150 Kapfenberg, Austria), and observed under a Quanta 250 scanning electron microscope  
151 (FEI, Eindhoven, Netherlands) at 15 kV.

152

### 153 2.3. *Determination of the antibacterial effect of chitosan*

154

155 *Enterococcus faecalis* (ATCC 29212) was cultured in Brain Heart Infusion broth (BHI,  
156 BioMérieux, Marcy-L'Etoile, France) at 37°C overnight. The bacterial suspension was  
157 then diluted in BHI to obtain concentrations of approximately  $2 \times 10^3$  Colony-Forming  
158 Units (CFU)/mL. The final bacterial solution was plated on agar plates after each  
159 experiment to ensure that the right bacterial concentration had been used. Fibrin-alone  
160 and fibrin-chitosan hydrogels were prepared as described above and cast in a 96-well  
161 plate (70  $\mu$ L per well). After gelation, 150  $\mu$ L of the bacterial suspension was added to  
162 the hydrogel-containing wells, as well as to empty wells for controls, and the plate was  
163 incubated at 37°C for 6 h. Bacterial suspensions were then harvested, diluted and plated  
164 on Trypticase Soy Agar (TSA; Biomérieux) with a EasySpiral automated plater  
165 (Interscience, Saint-Nom-la-Bretèche, France). CFUs were counted with a Scan 1200  
166 automated plate reader (Interscience) after plate incubation at 37°C for 18 h.

167

### 168 2.4. *Dental Pulp-Mesenchymal Stem/stromal Cell (DP-MSC) isolation and expansion*

169

170 Isolation and expansion of DP-MSCs were performed as described by Ducret et al. [33].  
171 Healthy impacted human third molars were collected from donors aged 13-17 years  
172 with informed consent of the patients and their parents, in accordance with the World  
173 Medical Association's Declaration of Helsinki and the French Public Health Code (Article  
174 R1211-49), and following a protocol approved by the French Ministry of Higher

175 Education and Research (CODECOH: DC-2014-2325). Dental pulps from teeth between  
176 Nolla developmental stages 5 (crown almost completed) and 7 (one third root  
177 completed) were gently extirpated from pulp cavities and cut into fragments of about  
178 0.5-2 mm<sup>3</sup>. Pulp fragments were seeded as explants on dishes pre-coated with a mixture  
179 of human placental collagens I and III at a final concentration of 0.5 µg/cm<sup>2</sup> and cultured  
180 in SPE-IV/EBM<sup>®</sup> medium. DP-MSCs outgrowing from the explants were passaged 4  
181 times before being encapsulated into the hydrogels. Our flow cytometry experiments  
182 revealed that the whole amplified cell population was positive to the MSC markers CD10,  
183 CD13, CD29, CD44, CD49a, CD73, CD90, CD105, CD166 and HLA-ABC. A significant  
184 percentage of these cells also expressed the mesenchymal stem cell antigen MSCA-1  
185 (about 50% of the cells), the marker of perivascular MSCs CD146 (15%), and the marker  
186 of neural and muscular MSCs CD56 (80%) [33,34,35].

187

## 188 2.5. *Preparation of cellularized hydrogels*

189

190 Fibrin-alone and fibrin-chitosan cellularized hydrogels were prepared by mixing DP-  
191 MSCs suspended in SPE-IV/EBM<sup>®</sup> medium with 80 mg/mL fibrinogen, 3 M sodium  
192 chloride, 0.4 M calcium chloride, PBS (for fibrin-alone hydrogels) or 1% chitosan (for  
193 fibrin-chitosan hydrogels) solutions and 4 U/mL thrombin, to get final concentrations of  
194 10 mg/mL fibrin, 0.5% chitosan and 5000 cells/µL into the hydrogels. Cell-containing  
195 formulations were immediately injected into the same plastic molds as above. Upon  
196 gelation, molds were placed in 24-well dishes and hydrogels were cultured in SPE-  
197 IV/EBM<sup>®</sup> medium for 7 days.

198

199 2.6. *Viability and morphological and ultrastructural characterization of DP-MSCs*  
200 *within hydrogels*

201

202 DP-MSC viability and morphological aspect were analyzed in fibrin-alone and fibrin-  
203 chitosan hydrogels, either immediately upon gelation or after 7 days of culture, with the  
204 Live/Dead® kit (Sigma-Aldrich) according to the manufacturer's instructions. For each  
205 condition (fibrin-alone and fibrin-chitosan), three cellularized hydrogels were performed with  
206 DP-MSCs cultured from 3 different third molars, each tooth originating from one different  
207 patient. Cellularized hydrogels were gently extruded from the molds, rinsed twice with  
208 PBS, and incubated in a PBS solution containing 0.2 µM calcein-AM and 0.2 µM PI at 37°C  
209 for 15 min. Hydrogels were then observed under a Nikon Eclipse TE300 fluorescence  
210 microscope, their most central region was photographed, and the percentage of living  
211 (green) cells was determined in a 200 square pixels' surface with the Image J software.

212 Cell ultrastructure and pericellular environment were analyzed with  
213 transmission electron microscopy. Fibrin-alone and fibrin-chitosan hydrogels  
214 cellularized with DP-MSCs were fixed after 7 days of culture in 2% glutaraldehyde  
215 diluted in 0.1 M sodium cacodylate buffer at RT for 4 h. After washing, samples were  
216 post-fixed in 1% osmium tetroxide for 1 h, dehydrated in a graded series of ethanol and  
217 embedded in Epon resin. After polymerization, ultrathin sections were cut with a  
218 diamond knife, picked up with copper grids (300-mesh), and post-stained with uranyl  
219 acetate and lead citrate on a Leica Ultrastainer. After air drying, grids were observed  
220 under a Philips CM 120 transmission electron microscope at an acceleration voltage of  
221 80 kV.

222

223 2.7. Cell proliferation and collagenous matrix production analysis with reverse  
224 transcription quantitative real-time polymerase chain reaction and immunohistochemistry  
225  
226 Expression of the genes coding for MKI67, the proliferation-related Ki-67 antigen, and  
227 for the alpha 1 chains of collagens type I and type III, two major structural components  
228 of the dental pulp ECM [36], was analyzed with reverse transcription quantitative real-  
229 time polymerase chain reaction (RT-qPCR) in DP-MSCs cultured in fibrin-alone or fibrin-  
230 chitosan hydrogels for 2, 4 or 7 days in SPE-IV/EBM® medium. Total RNA extraction was  
231 performed with the GenElute Single Cell RNA Purification kit (Sigma-Aldrich). Quality  
232 control of the extracted RNA was performed with 1µl samples by measuring UV  
233 absorbance (Thermo Scientific Nanodrop 2000, USA). The quantity of the extracted RNA  
234 was determined from the absorbance at 260 nm using a spectrophotometer (Nanodrop  
235 2000). RNA purity was determined from the ratio of absorbance ( $A@260/A@280$  nm  
236 and  $A@260/A@230$  nm >1.8 and <2.2). Equal amounts of total RNA (100 ng) were  
237 reverse-transcribed into single-stranded complementary DNA (cDNA) using the Prime  
238 Script RT reagent kit (Takara, Ozyme, Montigny-le-Bretonneux, France), in a T100  
239 thermal cycler (Bio-Rad, Hercules, CA, USA). Reverse transcription (RT) was performed  
240 using thermo-cycling conditions according to manufacturer's instructions: 37°C for 15  
241 min, 85°C for 10 s, and 4°C until further use or freezing. Quantitative real-time PCR  
242 (qPCR) amplifications were performed in a Rotor-Gene Q PCR cycler (Qiagen,  
243 Courtabœuf, France), in a 20 µL reaction mix containing 10µL Fast Start Universal SYBR  
244 green master (Roche, Mannheim, Germany), 4µL RT template diluted 1:3 in sterile  
245 water, 300 nmol/L of each primer, and 4µL sterile water. Thermal cycling conditions  
246 consisted of an initial denaturation step at 95° C for 10 min and then 40 to 50 cycles of  
247 95°C for 10 s, and a final annealing/extension step at 60° C for 20 s. The ribosomal

248 protein L13a housekeeping gene (*RPL13A*) was used for sample normalization. Primers  
249 for *MKI67* and *COL3A1* genes were designed using the Primer-Blast software  
250 (<http://www.ncbi.nlm.nih.gov/BLAST>). Primers for *COL1A1* and *RPL13A* were taken  
251 from publications [37,38]. Gene-specific primer sequences are listed in Table 1. All runs  
252 were performed in duplicate. The comparative threshold cycle method ( $\Delta\Delta C_t$ ) was  
253 employed for the relative quantification of gene expression. The expression level of each  
254 target cDNA marker was normalized to the *RPL13A* cDNA. Data were expressed as  
255 mRNA expression levels given by the  $2^{-(\Delta\Delta C_t)}$  method [39].

256       Detection of the proteins MKI67 and collagens type I and type III was performed  
257 in hydrogels cultured for 7 days by immunohistochemistry. Hydrogels were gently  
258 removed from the molds, fixed in acidified formal alcohol (AFA; Microm Microtech,  
259 Brignais, France) at RT for 24 h, dehydrated in ethanol, acetone and xylene and  
260 classically embedded in paraffin. Five-micrometer serial sections were then cut,  
261 deparaffinized and rehydrated. For MKI67 immunodetection, antigen retrieval was  
262 carried out by microwaving sections (230 watts) in pH 6, 10 mM citrate buffer for 20  
263 min. For collagen type I and collagen type III antigen retrieval, sections were incubated  
264 in 0.5% hyaluronidase diluted in PBS at RT for 1 h. After rinsing, sections were  
265 incubated with the anti-MKI67 rabbit recombinant monoclonal antibody (dilution 1/200  
266 in PBS-3% bovine serum albumin [BSA]), the anti-type I collagen rabbit polyclonal  
267 antibody (1/2000) or the anti-type III collagen mouse monoclonal antibody (1/2000) at  
268 4°C overnight. After rinsing in PBS, endogenous peroxidase activity was blocked by  
269 incubation in 0.5% hydrogen peroxide at RT for 20 min. Antibody detection was then  
270 performed by incubating sections with horseradish peroxidase-conjugated secondary  
271 antibodies diluted in PBS-3% BSA (anti-rabbit Dako EnVision+ System- HRP, ref. K4002,  
272 or anti-mouse Dako EnVision+ System- HRP, ref. K4000) at RT for 45 min. After rinsing

273 in PBS, the staining was revealed by incubating sections in the peroxidase substrate 3,3'-  
274 diaminobenzidine (DAB Substrate Chromogen System, ref. K3468; Dako-Agilent, Les  
275 Ulis, France) for 40-60 s. Sections were then slightly counterstained with Mayer's  
276 hematoxylin, mounted in aqueous medium and observed with a Leica DM2000 light  
277 microscope equipped with a DFC 450 camera. Images were acquired with the LASv4  
278 software. Staining controls were performed by replacing primary antibodies either with  
279 PBS -3% BSA or with rabbit or mouse control IgGs. All these controls were negative (not  
280 shown).

281

## 282 2.8. *Statistical analysis*

283

284 Data are presented as the mean values  $\pm$  standard deviation. Differences were analyzed  
285 using the Mann-Whitney U-test for nonparametric analysis. The number of independent  
286 samples from different donors (n) is indicated in figure captions. A *P* value < 0.05 was  
287 considered to be significant.

288

---

## 289 **3. Results**

290

### 291 3.1. *Preparation and characterization of the chitosan solution, fibrin hydrogels and* 292 *fibrin-chitosan hydrogels*

293

294 We first determined the concentrations of the chitosan solution that preserve a low  
295 viscosity of the final fibrin-chitosan formulation. This concentration was determined by  
296 measuring the viscosity of pH 7.2, 0.2-1% chitosan solutions. Our results showed that a  
297 chitosan concentration below 0.6% showed a relatively low viscosity (Fig. 1A). From this

298 value, the viscosity strongly increased. We then performed rheological measurements to  
299 determine whether the gelation time of fibrin-chitosan formulations with 0.1-0.5%  
300 chitosan concentrations was clinically acceptable. We found that, before fibrinogen  
301 polymerization, the viscoelastic moduli  $G'(t)$  and  $G''(t)$  remained low and relatively  
302 stable, and then both moduli increased and  $G'(t)$  became significantly higher than  $G''(t)$   
303 at longer times (Fig. 1B). The crossing point of the two curves provides an indication of  
304 the gelation time, in relation with the increasing number of physical junctions  
305 responsible for the formation of the fibrin gel network [40,41]. It was estimated here  
306 between 5 and 9 minutes, depending on the final concentration of chitosan entrapped  
307 into the fibrin network (Fig. 1C). Since all these times remained relevant to a clinical  
308 application, we decided to use for the remainder of the study the higher tested  
309 concentration of chitosan (0.5%) in the final formulation, in order to clearly exhibit the  
310 impact of the presence of chitosan in the final hydrogel.

311 Characterization of fibrin-alone hydrogels (Fig. 2A) with scanning electron  
312 microscopy after 7 days in SPE-IV/EBM<sup>®</sup> medium revealed a continuous network of  
313 fibrin fibrils (Fig. 2B). Chitosan addition resulted in the formation of rounded aggregates  
314 of chitosan entrapped in the fibrin network which was not altered (Fig. 2C and 2D).

315

316 *3.2. Determination of the antibacterial effect of chitosan incorporated into the fibrin*  
317 *hydrogel*

318

319 Bacterial growth was classically determined by counting CFUs after automated plating  
320 on agar plates (Fig. 3A and B). In the absence of hydrogel (control condition), *E. faecalis*  
321 mean final concentration was found to be  $4.60 \times 10^7$  CFU/mL after 6 h of incubation.  
322 When bacteria were grown with fibrin-alone hydrogels, the final bacterial concentration

323 was  $9.57 \times 10^7$  CFU/mL ( $p=0.0642$  versus control). When bacteria were grown with  
324 fibrin-chitosan hydrogels, their final concentration was significantly reduced ( $3.74 \times 10^6$   
325 CFU/mL) when compared to control or fibrin-alone conditions ( $p<0.0001$ ).

326

### 327 3.3. *Morphology, viability and proliferation of DP-MSCs cultured within hydrogels*

328

329 Encapsulated DP-MSCs were analyzed within either type of hydrogels, immediately after  
330 gelation or after 7 days of culture. At Day 0, living (green) DP-MSCs displayed a rounded  
331 morphology in fibrin-chitosan hydrogels (Fig. 4A), whereas, at Day 7, living cells were  
332 mostly elongated and fibroblast-like (Fig. 4B). Results were similar in fibrin-alone  
333 hydrogels (data not shown). The percentage of viable DP-MSCs (relative to the total  
334 number of DP-MSCs) was similar in fibrin-alone and fibrin-chitosan hydrogels, both at  
335 the beginning (Day 0) and at the end (Day 7) of culture (Fig. 4C). Cell proliferation was  
336 assessed by the expression of the nuclear marker MKI67 both at gene and protein level  
337 with RT-qPCR and immunohistochemistry, respectively. Compared to fibrin-alone  
338 hydrogels, *MKI67* gene expression was lower in fibrin-chitosan hydrogels after 2 days of  
339 culture but similar after 4 and 7 days of culture (Fig. 4D). The mean level of expression  
340 increased significantly between Day 2 and Day 4 of culture in fibrin-chitosan hydrogels.  
341 Proliferating cells were visualized after 7 days of culture by immunostaining of MKI67  
342 with a specific antibody. Only rare DP-MSCs were labelled in both fibrin-alone and  
343 fibrin-chitosan hydrogels (Fig. 4E and F).

344

### 345 3.4. *Ultrastructural characterization of DP-MSCs within hydrogels*

346



347 The capacity of viable DP-MSCs to produce ECM components in fibrin-alone (Fig. 5 A-D)  
348 and fibrin-chitosan hydrogels (Fig. 5 E-H) after 7 days of culture was then studied by  
349 transmission electron microscopy. The fibrin network was constituted by fibrils of  
350 different sizes (Fig. 5A). Chitosan formed rounded aggregates within the fibrin network  
351 (Fig. 5E). Special attention was paid to the cell cytoplasm in order to detect protein  
352 synthesis activity and to the close pericellular environment to determine whether cells  
353 were able to secrete collagenous components. Results indicated that DP-MSCs  
354 possessed, in both types of hydrogels, an abundant rough endoplasmic reticulum (Fig.  
355 5B, C, F and G). Collagen fibers, recognizable by their characteristic 67 nm periodic  
356 cross-striation, were observed in the pericellular environment (Fig. 5D and H).

357

### 358 3.5. *Collagenous matrix production by DP-MSCs within hydrogels*

359

360 Since collagens type I and type III are major structural components of the dental pulp  
361 ECM, we studied their expression by DP-MSCs in fibrin-alone and fibrin-chitosan  
362 hydrogels at both gene and protein level. Expression of genes coding for collagen type I  
363 and collagen type III alpha 1 chains (*COL1A1* and *COL3A1*) was analyzed with RT-qPCR  
364 after 2, 4 and 7 days of culture, and collagen type I and type III proteins were detected  
365 with immunohistochemistry after 7 days of culture. We found that *COL1A1* gene  
366 expression was significantly higher at Day 2 in fibrin-alone hydrogels compared to  
367 fibrin-chitosan hydrogels, but was similar at Day 4 and Day 7 (Fig. 6A). Collagen type I  
368 was immunolocalized close to DP-MSCs in both types of hydrogels (Fig. 6B and C).  
369 *COL3A1* gene expression was similar between both types of hydrogel at these same  
370 three time points (Fig. 6D). Collagen type III was also immunolocalized close to DP-MSCs  
371 after 7 days of culture (Fig. 6E and F).

372

---

373 **4. Discussion**

374

375 We report in this study the design and characterization of an innovative cellularized  
376 chitosan-supplemented fibrin hydrogel in a formulation which preserves chitosan  
377 antibacterial properties while promoting the formation of a DP-like connective tissue.

378 We first performed several tests to develop a chitosan solution of cytocompatible  
379 pH and sufficiently fluid to preserve the injectability of the final fibrin-chitosan  
380 formulation. Since the viscosity of a chitosan solution increases with polymer molar  
381 mass ( $M_w$ ), we selected shrimp shell chitosan with a  $M_w < 250$  kg/mol. To get a pH of the  
382 solution close to neutrality to avoid detrimental effects on cell viability, we were  
383 compelled to increase the pH of the solution after the acidic dissolution of chitosan in  
384 deionized water. We tested several batches of chitosans with 20%, 33% and 40% DA  
385 and we found that only the solution of chitosan with a 40%DA could be brought to pH  
386 neutrality without forming precipitates. This DA was accordingly selected for the rest of  
387 the study the results of which are reported here. We then assessed the viscosity of the  
388 chitosan-fibrin formulation and its gelation time. Indeed, a relatively low viscosity of the  
389 formulation is necessary to allow for easy injection into an emptied endodontic space  
390 with a millimeter range diameter, and an appropriate “setting time” is needed, not too  
391 fast to enable accurate injection of the formulation into the endodontic space and not too  
392 long to allow for the rapid implementation of the crown filling. Our results indicated that  
393 the viscosity of the DA40% chitosan solution remained moderated below a chitosan  
394 concentration of 0.6%. Above this value, viscosity sharply increased and no longer  
395 allowed for accurate hydrogel injection into the cylindrical-conical mold (not shown).  
396 Based on this finding, measurement of the time necessary to reach the gel point was

397 performed for different fibrin-chitosan hydrogels with chitosan concentrations varying  
398 from 0.1 to 0.5% w/w. Our results indicated that this time was ranging between 5 and 9  
399 minutes, which remained relevant to clinical application since it could allow slow  
400 injection of the formulation into the endodontic space of a one- to three-rooted human  
401 tooth. Accordingly, a final concentration of 0.5% chitosan was selected for the rest of the  
402 study.

403 The success of an endodontic treatment relies on the complete elimination of  
404 microorganisms present in the infected endodontic space. However, total disinfection  
405 can hardly be obtained with classical endodontic irrigants such as sodium hypochlorite,  
406 because of the complex anatomy of the root canal system and the limited penetrability of  
407 irrigants into the dentin tubules [42-44]. In this context, chitosan, given its known  
408 antibacterial properties, might be a good candidate to prevent the invasion of the fibrin  
409 scaffold by endodontic residual bacteria that could impair the DP regenerative process.  
410 In the field of dentistry, chitosan antibacterial effects have been assessed in the form of  
411 chitosan solutions, gels or nanoparticles mainly on *E. faecalis*, a pathogen highly  
412 resistant to endodontic disinfectants and which is frequently found in persistent root  
413 canal infections [26,27,45,46]. Our findings showed that incorporation of DA40%  
414 chitosan into the fibrin network was able to limit the growth of *E. faecalis* bacteria in  
415 contact with the hydrogel. Further experiments are needed (i) to test the antimicrobial  
416 activity of this scaffold against other bacteria present in the infected endodontic space,  
417 and (ii) to confirm that the chitosan can be released from the hydrogel to kill bacteria  
418 present either on the root canal dentin wall or in dentin tubules.

419 Tissue engineering studies have revealed that chitosan is highly biocompatible  
420 [47]. However, Kim et al. [48] have reported that chitosan alone did not significantly  
421 support human DP cell adhesion, proliferation or differentiation. The addition of

422 chitosan/hyaluronic acid or chitosan/pectin scaffolds to apical bleeding during  
423 revascularization procedures in dogs did not improve the regeneration of a pulp-dentin  
424 complex [14]. However, fibronectin/chitosan scaffolds were shown to promote DP stem  
425 cell attachment and proliferation [49], suggesting that chitosan association to  
426 fibronectin was not deleterious to the cells. In the present work we observed that  
427 addition of chitosan to a fibrin-based scaffold did not alter DP-MSC survival, spreading,  
428 proliferation, and collagenous matrix production. In particular, the level of cell viability  
429 was high and similar to that observed for mesenchymal stem cells, including DP-MSCs,  
430 seeded in a fibrin scaffold [9,10,50]. Based on *MKI67* gene expression, DP-MSC  
431 proliferation was significantly higher in fibrin-alone hydrogels than in fibrin-chitosan  
432 hydrogels after 2 days of culture, suggesting that chitosan limited cell proliferation at  
433 the beginning of the culture. Such limitation rapidly faded with time, because *MKI67*  
434 gene expression was similar in fibrin-alone and fibrin-chitosan hydrogels after 4 days of  
435 culture. The number of proliferative DP-MSCs was very low at Day 7 in both fibrin-alone  
436 and fibrin-chitosan hydrogels, suggesting that cells had begun to differentiate.

437         The morphology of DP-MSCs incorporated in both hydrogels was mostly  
438 elongated and spindle-like after 7 days of culture, close to that of DP fibroblasts [51].  
439 The early expression of collagen genes, soon after the beginning of cell culture within  
440 hydrogels, suggested that DP-MSCs in the fibrin-alone and fibrin-chitosan scaffolds were  
441 rapidly in favorable conditions to create a three-dimensional collagenous environment  
442 resembling their native tissue. Electron microscopy analysis after one week of culture  
443 indicated that cells were highly active, as shown by the presence of a well-developed  
444 rough endoplasmic reticulum and deposition of collagen fibers in the cell vicinity.

445         Together these results suggest that the association fibrin-chitosan in the form of a  
446 hydrogel could promote cell-based DP regeneration by maintaining a bacteria-free

447 environment in the endodontic space. They are in line with our recently published data  
448 reporting *ad integrum* regeneration of the colonic wall following implantation of fibrin-  
449 chitosan hydrogels cellularized with the stromal vascular fraction derived from the  
450 adipose tissue [52]. Cellularized fibrin-chitosan formulations could thus be used to  
451 regenerate various human tissues.

452

---

## 453 **5. Conclusion**

454

455 This study demonstrated that incorporating chitosan to a fibrin hydrogel confers the  
456 latter antibacterial properties which might prove helpful in endodontic space  
457 disinfection, without significantly altering the pro-regenerative properties of the fibrin  
458 scaffold. Further studies investigating this antibacterial effect should now be  
459 performed by using well-established monospecies or, better yet, multispecies biofilms  
460 similar to that present in the infected root canal. *In vivo* studies are also required to  
461 confirm these promising results and the interest of this scaffold for regenerative  
462 endodontics.

463

---

## 464 **Acknowledgements**

465 This work was supported by the *Gueules Cassées* foundation, the French National Centre  
466 for Scientific Research (CNRS) and the French Ministry of Higher Education and  
467 Research. The authors acknowledge the contribution of the *Centre Technologique des*  
468 *Microstructures* (Université Lyon 1, Villeurbanne, France) for help with electron  
469 microscopy and Novotec (Bron, France) for help with immunohistochemistry.

470

471 **REFERENCES**

---

472

- 473 [1] Ng YL, Mann V, Gulabivala K. Tooth survival following non-surgical root canal  
474 treatment: a systematic review of the literature. *Int Endod J* 2010;43(3):171-89.
- 475 [2] Kim SG, Zhou J, Ling L, Cho S, Suzuki T, Fu SY, et al. Regenerative endodontics:  
476 barriers and strategies for clinical translation. *Dent Clin North Am* 2012;56(3):  
477 639-49.
- 478 [3] Hargreaves KM, Diogenes A, Teixeira FB. Treatment options: biological basis of  
479 regenerative endodontic procedures. *J Endod* 2013;39(3):30-43.
- 480 [4] Rosa V, Zhang Z, Grande RH, Nör JE. Dental pulp tissue engineering in full-length  
481 human root canals. *J Dent Res* 2013;92(11):970-5.
- 482 [5] Diogenes A, Ruparel NB, Shiloah Y, Hargreaves KM. Regenerative endodontics. A  
483 way forward. *J Am Dent Assoc* 2016;147(5):372-80.
- 484 [6] Gong T, Heng BC, Lo ECM, Zhang C. Current advance and future prospects of  
485 tissue engineering approach to dentin/pulp regenerative therapy. *Stem Cells Int*  
486 2016;2016:9204574.
- 487 [7] Ducret M, Fabre H, Celle A, Mallein-Gerin F, Perrier-Groult E, Alliot-Licht B, et al.  
488 Current challenges in human tooth revitalization. *Biomed Mater Eng*  
489 2017;28(s1):S159-68.
- 490 [8] Nakashima M, Iohara K, Murakami M, Nakamura H, Sato Y, Ariji Y, et al. Pulp  
491 regeneration by transplantation of dental pulp stem cells in pulpitis: a pilot  
492 clinical study. *Stem Cell Res Ther* 2017;8(1):61.
- 493 [9] Galler K, D'Souza RN, Hartgerink JD, Schmalz G. Scaffolds for dental pulp tissue  
494 engineering. *Adv Dent Res* 2011;23(3):333-9.
- 495 [10] Galler KM, Brandl FP, Kirchhof S, Widbiller M, Eidt A, Buchalla W, et al. Suitability  
496 of different natural and synthetic biomaterials for dental pulp tissue engineering.  
497 *Tissue Eng Part A* 2018;24(3-4):234-44.
- 498 [11] Demarco FF, Conde MC, Cavalcanti BN, Casagrande L, Sakai VT, Nör JE. Dental  
499 pulp tissue engineering. *Braz Dent J* 2011;22(1):3-13.
- 500 [12] Rosa V, Della Bona A, Cavalcanti BN, Nör JE. Tissue engineering: from research to  
501 dental clinics. *Dent Mater* 2012;28(4):341-8.

- 502 [13] Jones TD, Kefi A, Sun S, Cho M, Alapati SB. An optimized injectable hydrogel  
503 scaffold supports human dental pulp stem cell viability and spreading. *Adv Med*  
504 2016;2016:7363579.
- 505 [14] Palma PJ, Ramos JC, Martins JB, Diogenes A, Figueiredo MH, Ferreira P, et al.  
506 Histologic evaluation of regenerative endodontic procedures with the use of  
507 chitosan scaffolds in immature dog teeth with apical periodontitis. *J Endod*  
508 2017;43(8):1279-87.
- 509 [15] Albuquerque MTP, Valera MC, Nakashima M, Nör JE, Bottino MC. Tissue-  
510 engineering-based strategies for regenerative endodontics, *J Dent Res*  
511 2014;93(12):1222-31.
- 512 [16] Janmey PA, Winer JP, Weisel JW. Fibrin gels and their clinical and bioengineering  
513 applications. *J R Soc Interface*. 2009;6(30):1-10.
- 514 [17] Ruangsawasdi N, Zehnder M, Weber FE. Fibrin gel improves tissue ingrowth and  
515 cell differentiation in human immature premolars implanted in rats. *J Endod*  
516 2014;40(2):246-50.
- 517 [18] Roura S, Gálvez-Montón C, Bayes-Genis A. Fibrin, the preferred scaffold for cell  
518 transplantation after myocardial infarction? An old molecule with a new life. *J*  
519 *Tissue Eng Regen Med* 2017;11(8):2304-13.
- 520 [19] Redl H, Schlag G, Stanek G, Hirschl A, Seelich T. In vitro properties of mixtures of  
521 fibrin seal and antibiotics. *Biomaterials* 1983;4(1):29-32.
- 522 [20] Fouad AF, Verma P. Healing after regenerative procedures with and without  
523 pulpal infection. *J Endod* 2014;40(4 Suppl):S58-64.
- 524 [21] Vishwanat L, Duong R, Takimoto K, Phillips L, Espitia CO, Diogenes A, et al. Effect  
525 of bacterial biofilm on the osteogenic differentiation of stem cells of apical papilla.  
526 *J Endod* 2017;43(6):916-22.
- 527 [22] Verma P, Nosrat A, Kim JR, Price JB, Wang P, Bair E, et al. Effect of residual  
528 bacteria on the outcome of pulp regeneration in vivo. *J Dent Res* 2017;96(1):100-  
529 6.
- 530 [23] Domard A. A perspective on 30 years research on chitin and chitosan.  
531 *Carbohydr Polym* 2011;84(2):696-703.
- 532 [24] LogithKumar R, KeshavNarayan A, Dhivya S, Chawla A, Saravanan S,  
533 Selvamurugan N. A review of chitosan and its derivatives in bone tissue  
534 engineering. *Carbohydr Polym* 2016;20(151):172-88.

- 535 [25] Raafat D, Sahi H-G. Chitosan and its antimicrobial potential - a critical literature  
536 survey. *Microb Biotechnol* 2009;2(2):186-201.
- 537 [26] Shenoi PR, Morey ES, Makade CS, Gunwal MK, Khode RT, Wanmali SS. In vitro  
538 evaluation of the antimicrobial efficacy of chitosan and other endodontic irrigants  
539 against *Enterococcus faecalis*. *Gen Dent* 2016;64(5):60-3.
- 540 [27] Shrestha, A, Kishen A. Antibacterial nanoparticles in endodontics: a review. *J*  
541 *Endod* 2016;42(10):1417-26.
- 542 [28] Husain S, Al-Samadani KH, Najeeb S, Zafar MS, Khurshid Z, Zohaib S, et al.  
543 Chitosan biomaterials for current and potential dental applications. *Materials*  
544 (Basel) 2017;10(6):602.
- 545 [29] Hosseinnejad M, Jafari SM. Evaluation of different factors affecting antimicrobial  
546 properties of chitosan. *Int J Biol Macromol* 2016;85:467-75.
- 547 [30] Montembault A, Viton C, Domard A. Physico-chemical studies of the gelation of  
548 chitosan in a hydroalcoholic medium. *Biomaterials* 2005;26(8):933-43.
- 549 [31] Dumont M, Villet R, Guirand M, Montembault A, Delair T, Lack S, et al. Processing  
550 and antibacterial properties of chitosan-coated alginate fibers. *Carbohydr*  
551 *Polym* 2018;190:31-42.
- 552 [32] Vachoud L, Zydowick N, Domard A. Formation and characterization of a physical  
553 chitin gel. *Carbohydr Res* 1997;302:169-77.
- 554 [33] Ducret M, Fabre H, Farges J-C, Degoul O, Atzeni G, McGuckin C, et al. Production of  
555 human dental pulp cells with a medicinal manufacturing approach, *J Endod*  
556 2015;41(9):1492-9.
- 557 [34] Ducret M, Fabre H, Degoul O, Atzeni G, McGuckin C, Forraz N, et al.  
558 Immunophenotyping reveals the diversity of human dental pulp mesenchymal  
559 stromal cells in vivo and their evolution upon in vitro amplification. *Front Physiol*  
560 2016;7:512.
- 561 [35] Ducret M, Fabre H, Degoul O, Atzeni G, McGuckin C, Forraz N, et al. A standardized  
562 procedure to obtain mesenchymal stem/stromal cells from minimally  
563 manipulated dental pulp and Wharton's jelly samples. *Bull Group Int Rech Sci*  
564 *Stomatol Odontol* 2016;53(1):e37.
- 565 [36] Goldberg M, Smith AJ. Cells and extracellular matrices of dentin and pulp: a  
566 biological basis for repair and tissue engineering. *Crit Rev Oral Biol Med*  
567 2004;15(1):13-27.



- 568 [37] Martin I, Jakob M, Schäfer D, Dick W, Spagnoli G, Heberer M. Quantitative analysis  
569 of gene expression in human articular cartilage from normal and osteoarthritic  
570 joints. *Osteoarthritis Cartilage* 2001;9(2):112-8.
- 571 [38] Pombo-Suarez M, Calaza M, Gomez-Reino JJ, Gonzalez A. Reference genes for  
572 normalization of gene expression studies in human osteoarthritic articular  
573 cartilage. *BMC Mol Biol* 2008;9:17.
- 574 [39] Livak KJ, Schmittgen TD. Analysis of relative gene expression data using real-time  
575 quantitative PCR and the  $2^{-\Delta\Delta C_T}$  method. *Methods* 2001;25(4):402-8.
- 576 [40] Stauffer D, Coniglio A, Adam M. Gelation and critical phenomena. *Adv Polymer Sci*  
577 1982;44(Polym. Networks):103-58.
- 578 [41] Montembault A, Viton C, Domard A. Rheometric study of the gelation of chitosan  
579 in aqueous solution without cross-linking agent. *Biomacromolecules* 2005;6(2):  
580 653-62.
- 581 [42] Shrestha A, Shi Z, Neoh KG, Kishen A. Nanoparticulates for antibiofilm treatment  
582 and effect of aging on its antibacterial activity. *J Endod* 2010;36(6):1030-5.
- 583 [43] Rosen E, Tsesis I, Elbahary S, Storzi N, Kolodkin-Gal I. Eradication of *Enterococcus*  
584 *fæcalis* biofilms on human dentin. *Front Microbiol* 2016;7:2055.
- 585 [44] Neelakantan P, Romero M, Vera J, Daood U, Khan AU, Yan A, et al. Biofilms in  
586 endodontics-Current status and future directions. *Int J Mol Sci* 2017;18(8). pii:  
587 E1748.
- 588 [45] Kishen A, Shi Z, Shrestha A, Neoh KG. An investigation on the antibacterial and  
589 antibiofilm efficacy of cationic nanoparticulates for root canal disinfection. *J*  
590 *Endod* 2008;34(12):1515-20.
- 591 [46] Ballal N, Kundabala M, Bhat K, Acharya S, Ballal M, Kumar R, et al. Susceptibility of  
592 *Candida albicans* and *Enterococcus fæcalis* to chitosan, Chlorhexidine gluconate  
593 and their combination in vitro. *Aust Endod J* 2009;35(1):29-33.
- 594 [47] Chedly J, Soares S, Montembault A, von Boxberg Y, Veron-Ravaille M, Mouffle C, et  
595 al. Physical chitosan microhydrogels as scaffolds for spinal cord injury  
596 restoration and axon regeneration. *Biomaterials* 2017;138:91-107.
- 597 [48] Kim NR, Lee DH, Chung PH, Yang HC. Distinct differentiation properties of human  
598 dental pulp cells on collagen, gelatin, and chitosan scaffolds. *Oral Surg Oral Med*  
599 *Oral Pathol Oral Radiol Endod* 2009;108(5):e94-100.

- 600 [49] Asghari Sana F, Çapkın Yurtsever M, Kaynak Bayrak G, Tunçay EÖ, Kiremitçi AS,  
601 Gümüşderelioğlu M. Spreading, proliferation and differentiation of human dental  
602 pulp stem cells on chitosan scaffolds immobilized with RGD or fibronectin.  
603 *Cytotechnology* 2017;69(4):617-30.
- 604 [50] Ho W, Tawil B, Dunn JC, Wu BM. The behavior of human mesenchymal stem cells  
605 in 3D fibrin clots: dependence on fibrinogen concentration and clot structure.  
606 *Tissue Eng* 2006;12(6):1587-95.
- 607 [51] Nancy A. Dentin-pulp complex. In: Nancy A, editor. *Ten Cate's Oral Histology:*  
608 *development, structure and function.* 8<sup>th</sup> edition. Elsevier Mosby, Saint-Louis, MO;  
609 2013, p. 165-204.
- 610 [52] Denost Q, Pontallier A, Buscail E, Montembault A, Bareille R, Siadous R, et al.  
611 Colorectal wall regeneration resulting from the association of chitosan hydrogel  
612 and stromal vascular fraction from adipose tissue. *J Biomed Mater Res A*  
613 2018;106(2):460-7.
- 614

615 **Table 1. Gene-specific primer sequences used for RT-qPCR analysis.**

616

Gene	Primer	Sequence	Amplicon size	Accession number
<i>MKI67</i>	Forward	5'-CGTCCCAGTGGAAGAGTTGT-3'	70 bp	NM_002417
	Reverse	5'-CGACCCCGCTCCTTTTGATA-3'		
<i>COL1A1</i>	Forward	5'-CAGCCGCTTCACCTACAGC-3'	83 bp	NM_000088.3
	Reverse	5'-TTTTGTATTCAATCACTGTCTTGCC-3'		
<i>COL3A1</i>	Forward	5'-TCAAGGCTGAAGGAAATAGCAA-3'	70 bp	NM_000090.3
	Reverse	5'-TCCCCAGTGTGTTTCGTGC-3'		
<i>RPL13A</i>	Forward	5'-AAAAAGCGGATGGTGGTTC-3'	168 bp	NM_012423.3
	Reverse	5'-CTTCCGGTAGTGGATCTTGG-3'		

617

618 **Figure legends**

619

620 **Figure 1 - Characterization of the chitosan solution and of fibrin-chitosan**  
621 **hydrogels.** (A) Determination of the viscosity of pH 7.2, 0.2-1% chitosan solutions. Values  
622 are the mean  $\pm$  standard deviation, n = 3. (B) An example of evolution of  $G'(t)$  and  $G''(t)$   
623 viscoelastic moduli in a fibrinogen-chitosan formulation containing 0.5% [w/w] chitosan.  
624 (C) Time necessary to reach the gel point for 0.1-0.5% chitosan concentrations in the  
625 fibrin-chitosan formulation. Values are the mean  $\pm$  standard deviation, n = 7.

626

627 **Figure 2 - Characterization of fibrin-alone and fibrin-chitosan hydrogels.** (A)  
628 Photograph showing an example of hydrogel (opaque white) cast in a cylindrical-conical  
629 transparent plastic mold (white arrow) and covered with SPE-IV/EBM® medium. (B)  
630 Scanning electron microscopy showing the continuous fibrin network in a fibrin-alone  
631 hydrogel. (C) Rounded aggregates of chitosan trapped between and around the fibrin  
632 fibrils in the fibrin-chitosan hydrogel. (D) High magnification of a chitosan aggregate.

633

634 **Figure 3 - Determination of the antibacterial effect of chitosan.** The effect of  
635 chitosan was determined by comparing the growth of *E. faecalis* bacteria in contact with  
636 fibrin-alone and fibrin-chitosan hydrogels. (A) Representative photographs of *E. faecalis*  
637 CFUs incubated at 37°C for 18 h on agar plates. The left picture shows CFUs obtained after  
638 the growth of bacteria in the absence of hydrogel (control). (B) Bacterial concentrations  
639 determined by CFU counting. Values are the mean  $\pm$  standard deviation, n = 3. \*p<0.0001.

640

641 **Figure 4 - Morphology, viability and proliferation of DP-MSCs cultured within**  
642 **hydrogels.** Representative picture of DP-MSCs in a fibrin-chitosan hydrogel stained with

643 the LiveDead kit® 2 h upon gelation (A; Day 0) and after 7 days of culture (B; Day 7). Dead  
644 cells were identified by the red nuclear staining resulting from the nuclear accumulation of  
645 propidium iodide. Viable cells were identified by the green cytoplasmic staining resulting  
646 from the cytoplasmic accumulation of calcein. (C) Percentage of viable DP-MSCs (relative  
647 to the total number of DP-MSCs). Values are the mean  $\pm$  standard deviation, n = 3. n.s.: not  
648 significant. (D) Expression of the proliferation marker gene *MKI67* in fibrin-alone and  
649 fibrin-chitosan hydrogels after 2, 4 and 7 days of culture. Values are the mean  $\pm$  standard  
650 deviation, n = 4. \*p<0.05. (E and F) Proliferating cells visualized after 7 days of culture by  
651 *MKI67* immunostaining.

652

653 **Figure 5 - Ultrastructural characterization of viable DP-MSCs and their pericellular**  
654 **environment within fibrin-alone and fibrin-chitosan hydrogels at Day 7.** (A) Fibrin  
655 fibrils. (B) Fibroblast-like DP-MSC with an elongated cellular process (arrow). N: nucleus.  
656 (C) DP-MSC cytoplasm showing a well-developed rough endoplasmic reticulum (RER). (D)  
657 Collagen fibers (arrows) in the pericellular environment. (E) Rounded chitosan  
658 aggregates (dark grey; two are indicated by black arrows) within the fibrin network. (F)  
659 Fibroblast-like DP-MSC with a well-developed rough endoplasmic reticulum. (G) Close  
660 contact between a DP-MSC and a chitosan aggregate. (H) Collagen fibers (arrows) in the  
661 pericellular environment.

662

663 **Figure 6 - Production of collagens type I and type III by DP-MSCs cultured in**  
664 **hydrogels.** (A and D) Expression of *COL1A1* and *COL3A1* genes by DP-MSCs in fibrin-  
665 alone and fibrin-chitosan hydrogels after 2, 4 and 7 days of culture. Values are the mean  $\pm$   
666 standard deviation, n = 4. \*p<0.05. Immunolocalization of collagens type I (B and C) and  
667 type III (E and F) in both types of hydrogels after 7 days of culture.

Figure 1

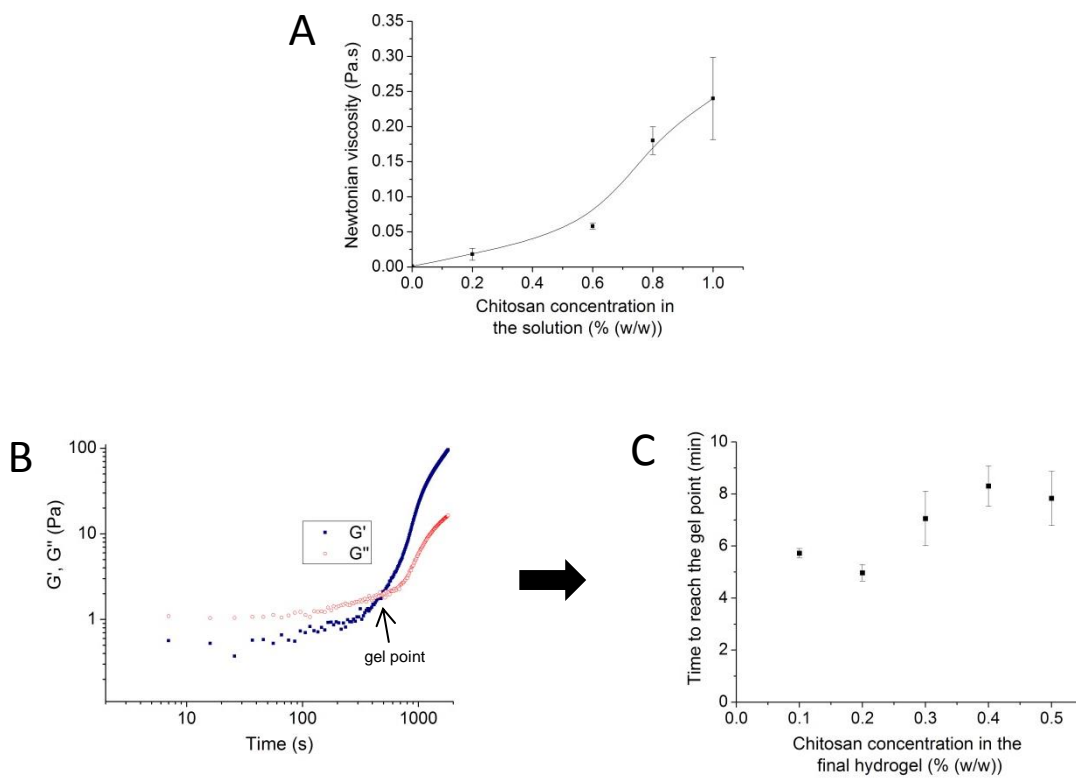


Figure 2

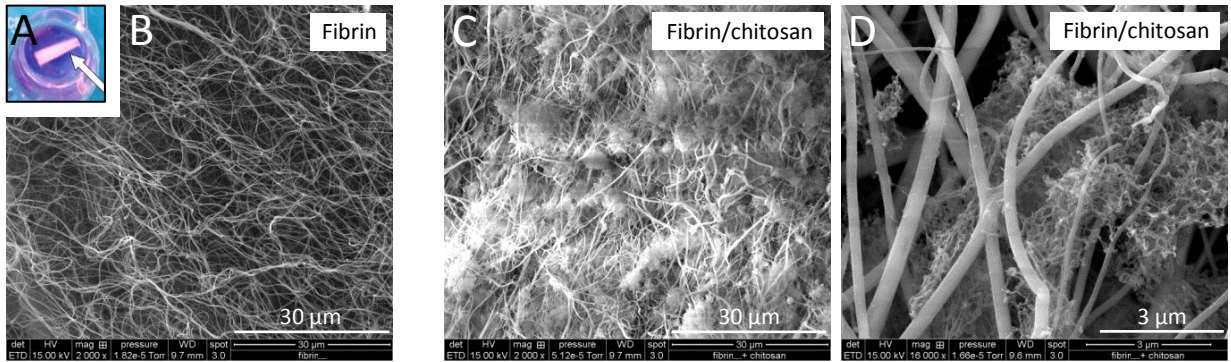
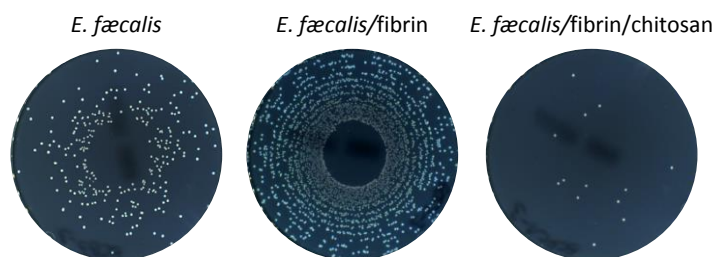


Figure 3

A



B

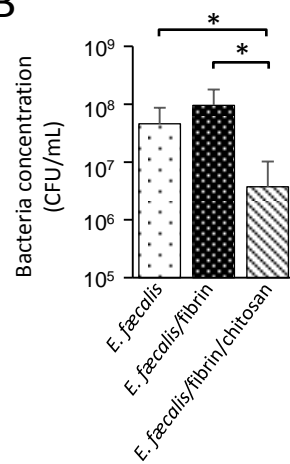




Figure 4

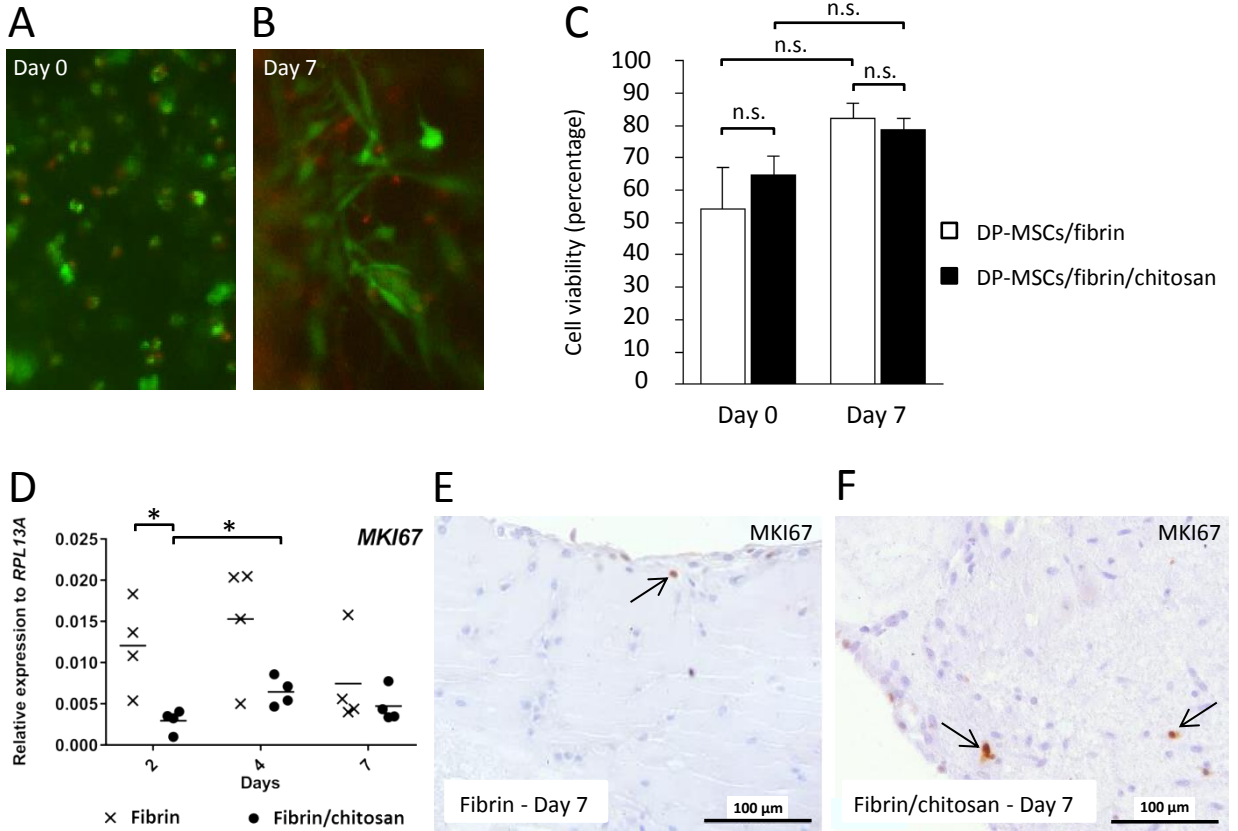
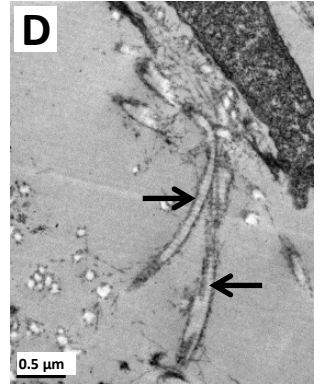
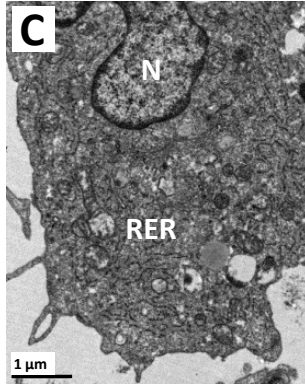
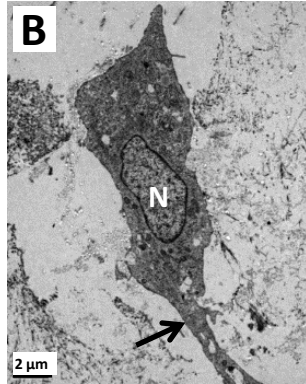
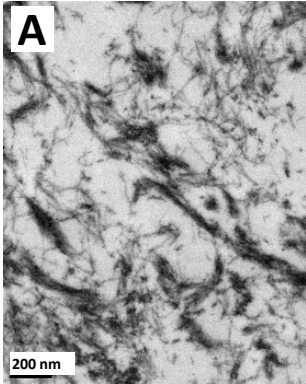


Figure 5

Fibrin



Fibrin/chitosan

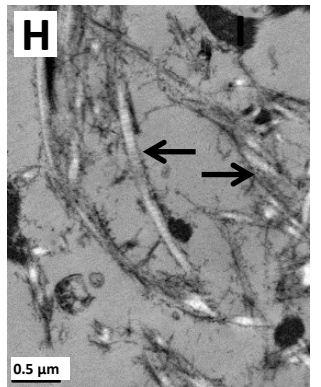
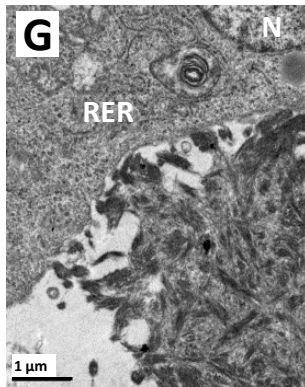
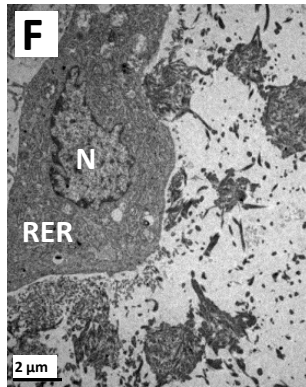
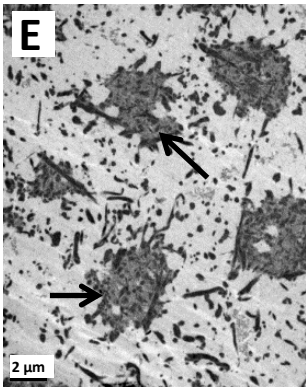


Figure 6

